1993ApJ...405..761T

THE ASTROPHYSICAL JOURNAL, 405:761–766, 1993 March 10
© 1993. The American Astronomical Society. All rights reserved. Printed in U.S.A.

DETECTION OF H_3^+ FROM URANUS

L. M. TRAFTON
Astronomy Department, University of Texas at Austin, Austin, TX 78712
T. R. GEBALLE
Joint Astronomy Center, 665 Komohana Street, Hilo, HI 96720
S. MILLER AND J. TENNYSON
Department of Physics and Astronomy, University College London, Gower Street, London, WC1E 6BT, UK
AND
G. E. BALLESTER
Department of Earth Sciences, University of Oxford, Parks Road, Oxford, OX1 3PR, UK
Received 1992 June 25; accepted 1992 September 16

ABSTRACT

The detection of H_3^+ in Uranus is reported. Using the CGS4 spectrometer on the UKIRT telescope, we clearly detected 11 emission features of the H_3^+ fundamental vibration-rotation band between 3.89 and 4.09 μm. These features are composed primarily of lines from the Q-branch; the strongest of them is the $Q(3)$ blend at 3.985 μm. Analysis of these features indicates a rotational temperature of 740 $\pm$ 25 K, an ortho-H_3^+ fraction of 0.51 $\pm$ 0.03, and a disk-averaged H_3^+ column abundance of 6.5×10^{10} ($\pm$10%) molecules cm^{-2}. Comparison is made with Jupiter (the only other planet for which H_3^+ has been detected), Saturn, and Neptune. A detection of the H_2 1–0 $S(1)$ line in Uranus and an upper limit to H_3^+ emission from Neptune also are reported. The rate of energy deposition into Uranus appears to be significantly higher than the rate reported during the *Voyager 2* flyby in January of 1986.

Subject headings: infrared: solar system — planets and satellites: individual (Uranus)

1. INTRODUCTION

Following the detection of near-infrared H_2 quadrupole emissions in Jupiter's polar spectra in 1986–1987 (Trafton et al. 1987, 1989a) and the detection of other K-band emission lines (Trafton, Lester, & Thompson 1989b), including the first overtone of H_3^+ (Drossart et al. 1989), Jupiter's near-infrared aurora has been the focus of intensive study. Since then, spectroscopic observations have revealed the fundamental H_3^+ band (Oka & Geballe 1990) and established thermal equilibrium for H_3^+, a rotational temperature in the neighborhood of 1000 K, and an ortho-H_3^+ fraction near 0.5 (Maillard et al. 1990; Miller, Joseph, & Tennyson 1990). Recently Jovian auroral arcs of H_3^+ emission in the L' band have been reported, from narrow-band imaging experiments by Baron et al. (1991) and Kim et al. (1991).

The presence of the auroral activity on Uranus was established by the detection of H_2 Lyman and Werner band as well as H Lyα localized nightside emissions by the Voyager Ultraviolet Spectrometer (Broadfoot et al. 1986). UV aurora on Uranus had first been postulated from the observation by the *International Ultraviolet Explorer* (*IUE*) of highly variable and strong H Lyα emission (cf. Clarke et al. 1986), although a significant part of this dayside emission is due to scattering and electroglow processes. The plasma science, cosmic-ray, and low-energy charged-particle experiments (Bridge et al. 1986; Stone et al. 1986; Krimigis et al. 1986) also detected a complement of magnetospheric electrons and protons, with H_2^+ as a minor constituent, but no H_3^+ was detected in contrast to the Jovian case.

The near-infrared wavebands, between 2 and 4 μm, have provided an alternative window for studying auroral phenomena on Jupiter. Ground-based observations of H_2 and H_3^+ are possible in the near-infrared, while spacecraft are needed to observe the UV aurora. Both UV and near-infrared emissions pertain to activity near and above the homopause of the planets. By contrast, the thermal hydrocarbon hot spots observed on Jupiter in the 8–13 μm window pertain to phenomena below the homopause (Halthore, Burrows, & Caldwell 1988; Kostiuk et al. 1990). Hence, the near-infrared region provides complementary access to the aeronomical physics and chemistry resulting from the magnetosphere-atmosphere interaction, in particular on the auroral ionospheric processes.

The main ion components in the ionospheres of the major planets are thought to be H^+ and H_3^+, but since the recombination rate of H_3^+ is uncertain (see Majeed & McConnell 1991), the abundance of this ion has been difficult to evaluate. Radio occultation experiments during spacecraft encounters measure the radial distribution of the ionosphere via the electron density, but these measurements do not provide the specific ion composition directly. Now, for the first time, we have remote H_3^+ observations that provide a direct measure of the ionospheric composition. The ionization results both from solar EUV input and from energetic charged particles occurring, for example, from auroral processes. Thus, H_3^+ observations serve as a diagnostic for these processes and also provide a new constraint for ionospheric modeling.

On Uranus the solar EUV has been thought to be the major ionization source producing the ionosphere observed from the radio-occultation experiment, because the auroral UV emissions detected by *Voyager* seemed so localized and weak (Strobel et al. 1991). Our H_3^+ detection now provides a new tool for studying not only the ionosphere in auroral and nonauroral regions, but also the relevance of the different magnetospheric processes.

Here we report the detection of H_3^+ in Uranus; this opens the door to ground-based studies of Uranium auroral/

© American Astronomical Society • Provided by the NASA Astrophysics Data System

1993ApJ...405..761T

ionospheric phenomena. We also report the detection of excited H_2 from Uranus and an upper limit to the H_3^+ emission from Neptune.

2. OBSERVATIONS

Spectra of Uranus near 4 μm were obtained on 1992 April 1 (UT) at the United Kingdom Infrared Telescope (UKIRT) in photometric conditions on Mauna Kea, using CGS4, the facility 1–5 μm cooled grating spectrometer, which currently houses a 58 × 62 InSb detector array. A 150 1/mm grating was used along with the 150 mm focal length camera, providing a pixel dimension of 3".1 on the sky. The slit width was also 3".1. The slit was oriented in the north-south direction. The spectral region covered was the portion of the L' band from 3.89 to 4.10 μm, and the resolving power of the instrument was approximately 1300, corresponding to a wavelength resolution of 0.0031 μm. Standard chopping and nodding techniques were employed during data acquisition. Wavelength calibration was obtained from a spectrum of an argon arc lamp in second order, and flux calibration was obtained from a spectrum of BS7264, assumed to have a blackbody shape with an L-magnitude of 1.76 and a temperature of 7000 K. The Brackett-α absorption line in the spectrum of this star was removed artificially prior to ratioing. All spectra were sampled every third resolution element.

Two spectra, slightly shifted in wavelength, were taken of Uranus, with total exposure times of 24 and 36 minutes between 0412 and 0600 UT. One row of the array was approximately centered on the disk of the planet. The resultant flux-calibrated spectra derived from this row were combined to produce the final spectrum shown in Figure 1. The final spectrum is smoothed by a Gaussian of FWHM half resolution element, which slightly lowers the resolution. The 1 σ noise level (per data point) of the spectrum ranges monotonically from 1×10^{-15} W m^{-2} μm at the short wavelength end to 2×10^{-15} W m^{-2} μm at the long wavelength end of the spectrum.

A spectrum of Neptune was obtained in photometric conditions on 1992 April 2 (UT), using CGS4 in the same configuration as for Uranus. The total exposure time was 58 minutes. Data reduction was similar to that described above; again BS 7264 served as the standard star.

A 2.05–2.15 μm spectrum of Uranus also was obtained in a brief measurement at dawn on 2 April in the "stare/nod" mode and with a resolving power of 1300. The spectrum indicated a marginal detection (S/N = 4) of the 1–0 S(1) line of H_2. A new spectrum, covering the same wavelength range, was obtained on 1992 May 5 and confirmed the detection of this line.

3. RESULTS

The spectrum of Uranus near 4 μm, displayed as flux versus vacuum wavelength in Figure 1, is a simple one, consisting only of emission lines. No continuum is present, except possibly at the long wavelength edge, presumably due to strong absorption of solar radiation by methane in the Uranian troposphere. This makes study of emission features considerably easier than for Jupiter or Saturn.

Eleven emission features due to lines of the H_3^+ fundamental ($v_2 \rightarrow 0$) are clearly detected in the spectrum of Uranus. In addition, there is a broad feature centered on 4.082 μm which coincides with several other H_3^+ lines of the fundamental band. The observed wavelengths, assignments, and fluxes are given in Table 1. All but one of the features [$P(1)$ at 4.070 μm] arise from the Q-branch of H_3^+. The strongest emission feature, centered at 3.985 μm, is due to the $Q(3)$ blend of two lines. Other strong features are at 3.953 μm [the $Q(1)$ line] and at 4.045 μm [the $Q(5)$ manifold].

At the time of the observations, the sub-Earth latitude on Uranus was −60.3 deg, and the equatorial diameter subtended

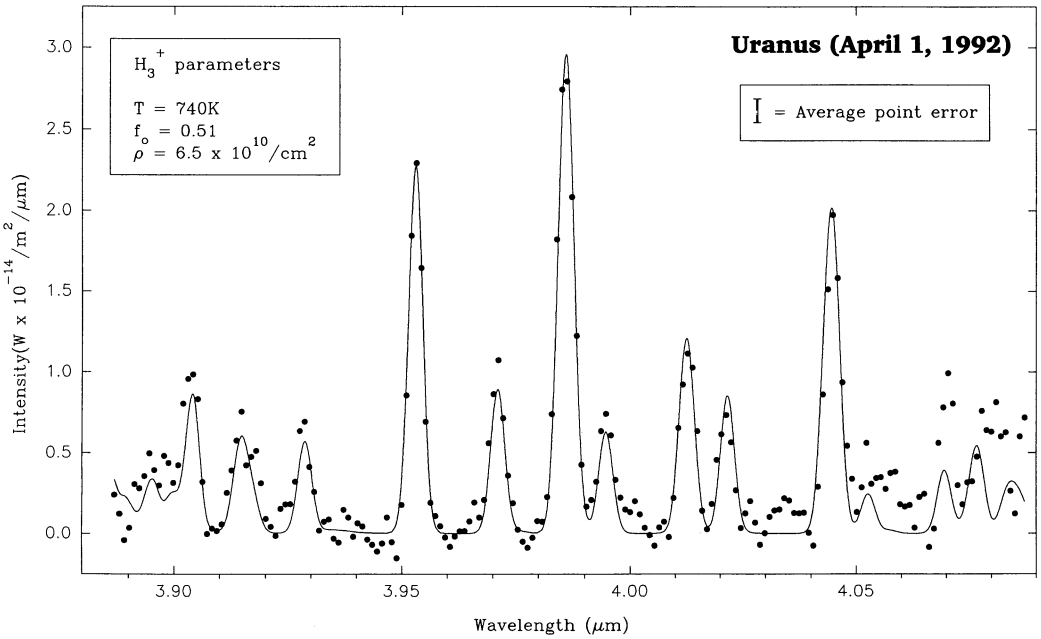

FIG. 1.—Spectrum of Uranus between 3.89 and 4.09 μm observed on 1992 April 1 (*filled circles*), compared with the fit obtained using the H_3^+ parameters reported (*solid line*). The resolution is approximately 0.0035 μm after the smoothing mentioned in the text; the spectrum is sampled every third resolution element. The error bar (± 1 σ) was estimated from the point-to-point variations in the baseline.

© American Astronomical Society • Provided by the NASA Astrophysics Data System

1993ApJ...405..761T

TABLE 1

H_3^+ LINE EMISSION FROM URANUS

Observed Peak Wavelength (μm)	Flux[a] (10^{-17} W m^{-2})	Peak S/N	Identification	Laboratory Wavelength (μm)
3.903	4.3 ± 0.4	4	3 3 +1 → 3 3	3.904
3.915	3.5 ± 0.4	3	2 2 +1 → 2 2	3.915
3.928	2.2 ± 0.4	3	1 1 +1 → 1 1	3.929
3.953	7.6 ± 0.4	10	1 0 −1 → 1 0	3.953
3.971	3.7 ± 0.4	5	2 1 −1 → 2 1	3.971
3.985	12.5 ± 0.5	20	3 0 −1 → 3 0	3.986
			3 1 −1 → 3 1	3.987
3.994	2.9 ± 0.4	5	3 2 −1 → 3 2	3.995
4.013	4.5 ± 0.5	7	4 1 −1 → 4 1	4.012
			4 2 −1 → 4 2	4.013
4.021	2.6 ± 0.5	4	4 3 −1 → 4 3	4.022
4.045	8.1 ± 0.6	7	5 2 −1 → 5 2	4.043
			5 3 −1 → 5 3	4.044
			5 1 −1 → 5 1	4.045
			5 0 −1 → 5 0	4.045
4.070	3.4 ± 0.6	3	0 1 +1 → 1 1	4.070
4.082[b]	3.7 ± 0.7	2	6 4 −1 → 6 4	4.076
			6 3 −1 → 6 3	4.077
			6 2 −1 → 6 2	4.082
			6 1 −1 → 6 1	4.085
			6 5 −1 → 6 5	4.087

[a] In a 3″.1 square aperture roughly centered on the planet. Uncertainties are based only on the noise level of the spectrum and not on the uncertainty in flux calibration, which is thought to be 10%.

[b] This is the central wavelength of a broad feature which may, in part, arise from H_3^+.

3″.57. The position angle of the visible south (IAU) rotational pole was 98.3 deg, and the pole was offset 0″.89 from the center of the disk. The solar phase angle was 2.9 deg. The strongest H_3^+ lines were marginally detected in each of the rows of the array adjacent to the central row, at about quarter the flux of the central row. If a similar amount of line radiation to the east and west of the slit also is missing from the central row spectrum, then the line fluxes from the entire Uranian disk are roughly twice the values listed in Table 1. The information in the adjacent rows was not used to derive the temperature or ortho H_3^+ fraction.

The apparent H_2 $S(1)$ emission flux in the May 5 spectrum of Uranus was 1.2×10^{-17} W m^{-2} in a 3″.1 square beam centered on the planet. The true emission flux is higher because the emission line is superposed on the quadrupole $S(1)$ absorption line. The 3–0 quadrupole H_2 lines, for example, are clearly visible in absorption in Uranus's spectrum (Trafton 1987). Discussion of the H_2 line emission is reserved for a later paper. No other emission features (e.g., the H_3^+ overtone line at 2.093 μm) were detected in the 2.05–2.15 μm region; upper limits are typically 3×10^{-18} W m^{-2} (2σ).

No lines were detected in the 3.9–4.1 μm spectrum of Neptune. The upper limits for narrow H_3^+ emission features, similar to those reported here in Uranus, are typically 5×10^{-18} W m^{-2}.

4. ANALYSIS

The spectrum shown in Figure 1 indicates that the continuum background radiation at 4 μm from Uranus is almost zero. On Jupiter, the tail of the P-branch of the ν_3 band of CH_4 is responsible for absorbing almost all the incoming solar radiation in the region around 4 μm. At latitudes above ~50 deg, peaks due to H_3^+ in the ionosphere are readily observable. Even at these higher latitudes, however, there remains a residual background due to incomplete absorption of the Sun's infrared spectrum (Miller et al. 1992a). On Uranus, it appears that the weaker insolation, coupled with a large concentration of tropospheric CH_4 compared to Jupiter (see Trafton 1987), results in a negligible background.

A model spectrum of H_3^+ was fitted to the observed spectrum of Uranus using the Einstein A_{if} coefficients given in Kao et al. (1991). The temperature, column density, and fraction of ortho-H_3^+ were used as free parameters. Figure 1 shows that the model spectrum accounts for the observed spectrum extremely well. The worst part of the fit is at wavelengths longer than about 4.07 μm, coinciding with the marginally detected $Q(6)$ lines of H_3^+, where the noise level is greatest and where there may be background radiation (not modeled) due to the reduced CH_4 absorption strength.

The fit to the spectrum implies a rotational temperature of $T = 740 \pm 25$ K, an ortho-H_3^+ fraction of 0.51 ± 0.03 and a vertical column density of 6.5×10^{10} cm^{-2} ± 10% allowing for the secant brightening effect in calculating the average column density over the entire planetary disk. Assuming a near-thermal population of upper energy levels, our H_3^+ parameters are consistent with a flux due to this ion of 0.030 ergs s^{-1} cm^{-2}, which assumes the observed flux is uniformly distributed over the disk (The dimensions of the source region on Uranus are unknown). The fit to the Uranus observed spectrum indicates a total of 5.3×10^{30} H_3^+ molecules were present in the 3″.1 square beam. If LTE is assumed, the total luminosity in infrared H_3^+ lines from these molecules is approximately 2.5×10^{11} W. As discussed earlier, these values probably should be multiplied by a factor of 2 to obtain the totals for the entire disk; that is, 1.1×10^{31} H_3^+ molecules and 5×10^{11} W.

5. DISCUSSION

5.1. *Physical Conditions in the Uranian Emission Region*

Assuming a 10% conversion rate, we find that the H_3^+ emissions indicate 2.5×10^{12} W of power are being deposited in the upper atmosphere of Uranus in the area covered by our spectroscopic slit. This value must then be considered a lower limit for the total energy deposited over the entire planet, because our beam did not quite cover Uranus's disk and we have no information about the back side. This compares with the value estimated from the *Voyager* UV experiment for the total auroral energy deposition for Uranus's dark pole of 0.2×10^{12} W, or for the dayside electroglow of 0.17×10^{12} W (Broadfoot et al. 1986). Recent reanalysis of the *Voyager* UV pre- and postencounter observations for Uranus (Herbert & Sandel 1991) shows that the dayside aurora is at least comparable in brightness to the darkside aurora. Therefore, the UV input power at the *Voyager* epoch could well have been $\sim 0.4 \times 10^{12}$ W. We conclude that the energy deposition rate into Uranus appears to be more than 6 times greater than found during the *Voyager 2* flyby in January of 1986.

The temperature of 740 K we report for H_3^+ in the atmosphere of Uranus is somewhat cooler than is normal for H_3^+ in Jupiter's atmosphere, but there are occasions when Jupiter's H_3^+ gets this cool, judging from the occasional weakening of the overtone spectrum relative to the fundamental (e.g., Oka & Geballe 1990). This appears to have been the case for spectra of Jupiter taken on the same night as our Uranus spectra (Miller et al. 1992c). The above temperature, derived from the 4 μm spectrum of Uranus, is consistent with the lack of detection of

© American Astronomical Society • Provided by the NASA Astrophysics Data System

1993ApJ...405..761T

the H_3^+ overtone emission on Uranus. An initial analysis of echelle spectra of the north polar region of Jupiter taken on 1992 April 9 (UT) using the NASA Infrared Telescope Facility indicates that the Jovian polar H_3^+ may have been as cold as 600 K (Miller et al. 1992b). Therefore, the energetics of the excitation process in the Uranian atmosphere may be comparable to that in the larger, Io-pumped Jovian magnetosphere.

The 740 K temperature is also comparable to the temperature of Uranus's upper atmosphere (Herbert et al. 1987) including the region of the ionosphere and hydrogen corona (Lindal et al. 1987). Recent models by Majeed & McConnell (1991) of the ionospheres of Jupiter and Saturn, also applicable to Uranus, favor an upper ionosphere consisting of H^+; this would be consistent with the observations for Uranus (Strobel et al. 1991). These models also favor a lower ionosphere containing H_3^+. The *Voyager* radio occultation experiment measured electron densities of $\sim 10^3$ cm^{-3} in the lower levels of the Uranian ionosphere during egress (the ingress data showed even higher densities). Even if the lower H_3^+ region of the extensive ($\sim$10,000 km) Uranian ionosphere were as thin as $\sim$1000 km, the ion column densities should be more than adequate to produce the 6.5×10^{10} cm^{-2} H_3^+ column density derived from our observations.

Drossart et al. (1989) have suggested that the ortho-H_3^+ fraction in Jupiter may reflect the temperature of the molecular hydrogen from which the H_3^+ is formed; while para-H_2 can only form para-H_3^+, ortho-H_2 forms two-thirds ortho-H_3^+ and one-third para-H_3^+ (Quack 1977). At room temperatures, the equilibrium fraction of ortho-H_2 is 0.75, and that of para-H_2 0.25. This gives rise to a fraction of ortho-H_3^+, $f_0 = 0.5$. However, the ground rotational state ($j = 0$) of H_2 is para-H_2, and this is preferred at low temperatures. The equilibrium fraction of ortho-H_2 is then considerably less than 0.75 and depends on the exact temperature. In this case, if no equilibrium takes place after the formation of H_3^+, the value of f_0 for H_3^+ will be less than 0.5.

Low temperatures are expected in the Uranian stratosphere (62 K at the 10 mbar level; 160–170 K at the 3 μbar level; Hanel et al. 1986; French et al. 1983). At 62 K the equilibrium fraction of para-H_2 is 0.65; at 160 K it is 0.28, close to the value one-quarter corresponding to room temperature and higher. The observed H_3^+ emission is expected to arise from atmospheric regions above Uranus's deep homopause, where diffusive separation occurs (located at the fractional mbar level, where temperatures are in excess of 100 K; Bishop et al. 1990), because protonation of hydrocarbons is an important sink for H_3^+. The observed value of Uranus's ortho-H_3^+ fraction of 0.51 ± 0.03 suggests formation of H_3^+ is occurring in the regions where H_2 has equilibrated at a temperature of 150 K or higher; that is, above the 10 μbar level.

5.2. *Comparison with Other Planets*

The intensity of Uranus's H_3^+ emissions and the computed column density are a few percent of those of the Jovian aurora (Miller et al. 1992a). This is not inconsistent with the 14 times less solar wind intensity and insolation at Uranus, which is 3.7 times farther from the Sun than Jupiter is. However, if the H_3^+ emissions follow the UV auroral emissions, which are sharply localized near the magnetic poles (Broadfoot et al. 1986; Herbert & Sandel 1991), the peak intensity and column abundance could well be comparable with those measured in Jupiter. Another possibility is that at least part of the H_3^+ emissions are due to emission by this ion which may be present in Uranus's hot, extended ionosphere ($T \sim 800$ K; Strobel et al. 1991).

A significant difference between Uranus and Jupiter occurs in the colatitude of the magnetic poles. The Jovian magnetic pole is tilted with respect to the spin axis only by 10 deg, while the Uranian magnetic dipole is tilted 60 deg with respect to the spin axis, toward 48 deg W longitude (Ness et al. 1986). In this configuration, Uranus's equatorial satellites sweep out larger volumes of the magnetosphere than do Jupiter's satellites (Krimigis et al. 1986). However, this is evidently not enough to quench the Uranian auroral phenomena as evidenced by the detection of UV aurora.

Since this work was completed, Geballe, Jagod, & Oka (1992) have reported the detection H_3^+ emission from Saturn. They found intensity levels weaker than reported here for Uranus. Given the level of UV auroral activity on Saturn, this poses something of a puzzle. On Jupiter, to explain the lack of H_3^+ emission around longitude 180 deg in the north aurora where the UV emission usually peaks, Ballester et al. (1991) have proposed that since at these longitudes the energy is deposited in deeper hydrocarbon levels (Livengood, Strobel, & Moos 1990), the H_3^+ is quickly destroyed by reactions with hydrocarbons (Yung & Strobel 1980). This may have implications on the detection of H_3^+ emission on Uranus and on the difficulty of detection on Saturn (R. Prangé 1992, private communication). Compared to Jupiter and Saturn, Uranus's homopause is very deep due to its low eddy diffusion coefficient ($< 10^2$ cm^2 s^{-1}; Yelle et al. 1989; Bishop et al. 1990; Ben Jaffel et al. 1991). The auroral energy deposition, as found in our H_3^+ observations and the UVS detection (Broadfoot et al. 1986), occurs above the hydrocarbon homopause. On the contrary, Saturn has a large eddy diffusion coefficient ($> 5 \times 10^6$; Smith et al. 1983), and thus a high homopause (in the fractional μbar levels). Sandel et al. (1982) reported that Saturn's brightest UV aurorae show absorption by CH_4; that is, the particles are penetrating the hydrocarbon levels, but they also report that the weakest aurorae do not show any CH_4 absorption and should originate near the exobase. It is therefore possible, but not entirely clear, that Saturn's higher homopause might interfere with the production of H_3^+. More studies are needed for a proper assessment.

5.3. *Spatial Distribution of Line Intensity*

Since the current sub-Earth latitude is -60 deg and Uranus's northern magnetic pole lies at latitude -15 deg (in the IAU frame), the magnetic pole moves between one-half of Uranus's disk radius to the apparent limb. It is visible $\sim$60% of the time. The southern magnetic pole is not visible. The position angle of Uranus's magnetic pole is uncertain owing to the uncertainty in the 17.24 ± 0.01 hr rotational period of Uranus's magnetosphere, which was determined during the *Voyager* flyby over 6 years ago (Desch, Connerney, & Kaiser 1986). We cannot determine whether Uranus's magnetic pole was in plain view during our H_3^+ observations.

Also, the dipole is offset 30% from the planet's center causing a variation over the surface of the magnetic field strength from a minimum of 0.1 G on the sunlit side to 1.1 G near the night magnetic pole. Hence, the mirror points should lie closer to the surface near the northern magnetic pole so one would expect auroral phenomena to be favored on the side of Uranus facing the Earth. This suggests that the H_3^+ emission should be concentrated near this pole. Herbert & Sandel (1991) reported auroral emission near the N (sunlit) magnetic pole

© American Astronomical Society • Provided by the NASA Astrophysics Data System

1993ApJ...405..761T

from analysis of the global data obtained by the *Voyager 2* UVS experiment; however, this question is currently being reassessed (F. Herbert 1992, private communication). Meanwhile, our H_3^+ observations may be an indication of the presence of the northern aurora.

6. CONCLUSION

This reports the detection of H_3^+ line emission from Uranus and sets an upper limit to the emission intensity for Neptune. H_3^+ emission from Uranus is considerably stronger than that from either Saturn or Neptune. The temperature of the H_3^+ emission on Uranus appears to be somewhat cooler than is typical in the Jovian aurora. Interpretation of the column abundance (as well as the observed flux in terms of the true intensity) is limited by our lack of the knowledge of the true source area, although more recent measurements by T. R. Geballe, M. F. Jagod, and T. Oka (T. R. Geballe, 1992, private communication) at a spatial resolution of 1".5 and 1" seeing indicate that the north-south intensity of the emission is roughly constant across the planet.

At this point, the role played by H_3^+ on Jupiter, for which considerably more data is available, is not clear. Some imaging of the planet indicates that the H_3^+ aurorae do not correlate well with the loci of ultraviolet aurorae derived from *Voyager* measurements in 1979 (Baron et al. 1991), although this is questioned by other data (Kim et al. 1991). However, the recent new images of Jupiter aurora in the Lyα emission, obtained with the *Hubble Space Telescope*, have revealed structure that seems to be more correlated to the H_3^+ distribution (Dols et al. 1992). This issue addresses the question about the magnetospheric processes responsible for producing the Jovian aurorae, and whether H_3^+ emission is the signature of a process different from that which causes UV emission.

Baron et al. (1991) have also presented evidence to show some anticorrelation between the H_3^+ aurorae and "hot spots" due to hydrocarbon emission. This in turn raises the question as to the link between processes in the ionosphere and those occurring at higher densities below the homopause. H_3^+ is known to be very reactive, acting as a protonating agent for many reactions and as a source of hydrogen atoms. It may be that the hydrocarbon "hot spots" occur in regions where H_3^+ formation is occurring at a level in the atmosphere where heavier elements are also present—for reasons for which there is no generally accepted explanation—and that subsequent reactions are destroying the H_3^+ but activating hydrocarbon chemistry.

Miller et al. (1992a) have drawn attention to the role of H_3^+ in the energy balance of the upper atmosphere of Jupiter, showing that the cooling effect of its emissions may vary considerably from day to day. They have also shown that there are large variations in column density and temperature from location to location on the planet.

These, and other, observations of Jupiter all point to H_3^+ as an important source of information about spatial and temporal variations in energy input and output in planetary ionospheres, providing data which can both inform and constrain models of magnetosphere/ionosphere interactions and the chemistry of the upper atmosphere. Although obtaining the same quality of data for Uranus will obviously be more difficult than for the nearer and brighter Jupiter, this paper indicates that Uranus will be a rich source of information.

Future observations will focus on the resolution of the spatial extent of the H_3^+ emission, to determine the relative importance of the auroral and nonauroral processes. However, the temporal behavior of the emission is also of interest in terms of the visibility of the auroral region. Resolution of the spatial distribution and temporal behavior of the H_3^+ emissions may prove particularly important for the auroral studies on Uranus since the only other method for presently studying Uranus's upper atmospheric phenomena, FUV observations, is severely limited. Since only H Lyα is detectable, one would have to wait for a new generation of much more sensitive UV-imaging instruments. It is clear that this detection of H_3^+ on Uranus has enormously increased the potential for ground-based studies of the planet's upper atmosphere.

L. M. T. acknowledges the support of NASA grant NAGW-2314. S. M. and J. T. acknowledge support from SERC under grant GR/G/15512. R. Prangé, D. F. Strobel, and D. Flower are thanked for their helpful communications. We thank the staff of UKIRT for its assistance with these observations.

REFERENCES

Ballester, G. E., Prangé, R., Kim, S., Livengood, T., Moos, H. W., & Caldwell, J. 1991, BAAS, 23, 1133
Baron, R., Joseph, R. D., Owen, T., Tennyson, J., Miller, S., & Ballester, G. E. 1991, Nature, 353, 539
Ben Jaffel, L., Prangé, R., Emerich, C., Vidal-Majar, A., & McConnell, J. C. 1991, J. Geophys. Res., 96, 9781
Bishop, J., Atreya, S. K., Herbert, F., & Romani, P. 1990, Icarus, 88, 448
Bridge, H. S., et al. 1986, Science, 233, 89
Broadfoot, A. L., et al. 1979, Science, 204, 979
———. 1986, Science, 233, 74
Clarke, J. T., et al. 1986, J. Geophys. Res., 91, 8771
Desch, M. D., Connerney, J. E. P., & Kaiser, M. L. 1986, Nature, 322, 42
Dols, V., Gerard, J. C., Paresce, F., Prangé, R., & Vidal-Majar, A. 1992, Geophys. Res. Lett., in press
Drossart, P., et al. 1989, Nature, 340, 539
Drossart, P., Prangé, R., & Maillard, J. P. 1992, Icarus, 97, 10
French, R. G., et al. 1983, Icarus, 53, 399
Geballe, T. R., Jagod, M.-F., & Oka, T. 1992, IAU Circ., No. 5566
Halthore, R., Burrows, A., & Caldwell, J. 1988, Icarus, 74, 340
Hanel, R., et al. 1986, Science 233, 70
Herbert, F., & Sandel, B. R. 1991, BAAS, 23, 1147
Herbert, F., Sandel, B. R., Yelle, R. V., Holberg, J. B., Broadfoot, A. L., & Shemansky, D. E. 1987, J. Geophys. Res., 92, 15, 093
Kao, L., Oka, T., Miller, S., & Tennyson, J. 1991, ApJS, 77, 317
Kim, S. J., Drossart, P., Caldwell, J., Maillard, J. P., Herbst, T., & Shure, M. 1991, Nature, 353, 536
Kostiuk, T., Espenak, F., Romani, P., & Goldstein, J. 1990, BAAS, 22, 1066
Krimigis, S. M., et al. 1986, Science, 233, 97
Lindal, G. F., Lyons, J. R., Sweetnam, D. N., Eshleman, V. R., Hinson, D. P., & Tyler, G. L. 1987, J. Geophys. Res., 92, 14987
Livengood, T. A., Strobel, D. F., & Moos, H. W. 1990, J. Geophys. Res., 95, 10375
Maillard, J. P., Drossart, P., Watson, J. K. G., Kim, S. J., & Caldwell, J. 1990, ApJ, 363, L37
Majeed, T., & McConnell, J. C. 1991, Planet. Space. Sci., 39, 1715
Miller, S., Joseph, F. D., Lam, H. Ridgway, S., & Tennyson, J. 1992a, ApJ, submitted
Miller, S., Joseph, R. D., & Tennyson, J. 1990, ApJ, 360, L55
Miller, S., Lam, H., Joseph, R. D., Tokunaga, A., & Tennyson, J. 1992b, in preparation
Miller, S., Trafton, L. M., Geballe, T. R., Simon, T., Lam, H., Tennyson, J., & Ballester, G. E. 1992c, in preparation
Ness, N. F., Acuna, M. H., Behannon, K. W., Burlaga, L. F., Connerney, J. E. P., Lepping, R. P., & Neubauer, F. M. 1986, Science, 233, 85
Oka, T., & Geballe, T. R. 1990, ApJ, 351, L53
Quack, M. 1977, Molec. Phys., 34, 477
Sandel, B. R., et al. 1982, Science, 215, 458
Smith, G. R., Shemansky, D. E., Holberg, J. B., Broadfoot, A. L., Sandel, B. R., & McConnell, J. C. 1983, J. Geophys. Res., 88, 8667
Stone, E. C., et al. 1986, Science, 233, 93
Strobel, D. F., Shemansky, D. E., Yelle, R. V., & Atreya, S. K. 1991, in Uranus, ed. J. T. Bergstralh, E. D. Miner, & M. S. Matthews (Tucson: Univ. Arizona Press), 65
Trafton, L. M. 1987, Icarus, 70, 13

© American Astronomical Society • Provided by the NASA Astrophysics Data System

1993ApJ...405..761T

Trafton, L. M., Carr, J., Lester, D. F., & Harvey, P. 1987, Icarus, 74, 351
———. 1989a, in Time Variable Phenomena in the Jovian System, ed. M. J. Belton, R. A. West, & J. Rahe (NASA SP-494), 229
Trafton, L. M., Lester, D. F., & Thompson, K. L. 1989b, ApJ, 343, L73
Yelle, R. V., McConnell, J. C., Strobel, D. F., & Doose, L. R. 1989, Icarus, 77, 439
Yung, Y. L., & Strobel, D. F. 1980, ApJ, 239, 395

© American Astronomical Society • Provided by the NASA Astrophysics Data System